ELSEVIER

Respiratory Physiology & Neurobiology 132 (2002) 329–339

RESPIRATORY PHYSIOLOGY & NEUROBIOLOGY

www.elsevier.com/locate/resphysiol

Axial and radial distribution of the bronchial vasculature in sheep

Joseph C. Anderson [a], Susan L. Bernard [b], Daniel L. Luchtel [c], Albert L. Babb [a], Michael P. Hlastala [b,d,*]

[a] *Department of Chemical Engineering, University of Washington, Seattle, WA 98195, USA*
[b] *Department of Medicine, Division of Pulmonary and Critical Care Medicine, University of Washington, Box 356522, Seattle, WA 98195-6522, USA*
[c] *Department of Environmental Health, University of Washington, Seattle, WA 98195, USA*
[d] *Department of Physiology and Biophysics, University of Washington, Box 356522, Seattle, WA 98195-6522, USA*

Accepted 29 May 2002

Abstract

A morphometric analysis was made on the bronchial vasculature of intrapulmonary airways in sheep lungs. This study provides the parameters to calculate the quantity of soluble gas diffusion between the vasculature and airways for use in a mathematical model describing heat and mass exchange in the lungs. To achieve these results, the lungs of four adult sheep (30–36 kg.) were excised, fixed, dissected and microtomed to obtain airway cross-sections for measurement. Blood vessel size and airway proximity was measured using a microscope interfaced with a computer. Distance from airway lumen to most airway vessels ranged from 30 to 270 μm. It was found that the bronchial vessels surrounding intraparenchymal airways can be described by a right-skewed distribution. Most importantly, a practical description of the bronchial capillary size and airway proximity as a function of airway diameter was found using a weighed average. This analysis facilitates calculation of soluble gas flux from the bronchial vasculature to the airway for use in a mathematical model.

Keywords: Airways, heat and mass exchange; Bronchial circulation, morphometry; Mammals, sheep; Models, heat and mass exchange in lung

1. Introduction

Although tiny and unsung, the bronchial circulation plays an important role in many lung processes. In health, it acts as 'the nutritive vessels of the lung (Cudkowicz, 1992)'. The pulmonary nerves, connective tissue and muscle surrounding the airways are all supported by this circulation. It rehydrates mucus desiccated from normal breathing and plays an active role in thermoregulation (Baile et al., 1985). The bronchial circulation can eliminate highly soluble gases (i.e. ethanol) and participate in airway clearance of soluble aerosols (Rizk et al., 1984). In disease or

* Corresponding author. Tel.: +1-206-543-3166; fax: +1-206-685-8673
E-mail address: hlastala@u.washington.edu (M.P. Hlastala).

1569-9048/02/$ - see front matter
PII: S1569-9048(02)00078-2

injury, the bronchial circulation has been described as the 'Red Cross' of the lung (Deffebach et al., 1987). With inflammation or asthma, the circulation hypertrophies and recruits vessels to begin the healing process (Charan et al., 1997). Additionally, it can perform limited respiratory gas exchange if the pulmonary circulation fails (Charan and Carvalho, 1997).

Fundamental to understanding the physiological role of the bronchial microcirculation is understanding its anatomy. Investigators have studied many facets of the bronchial circulation. Pump (1972), Magno and Fishman (1982) have described the circulation's gross anatomy in humans and sheep, respectively. Others have searched for bronchopulmonary anastomoses (Charan et al., 1984; Schraufnagel et al., 1995). Still other investigators have given a three dimensional description (Hill et al., 1989; Laitinen et al., 1989). In all, the studies have been mainly qualitative in nature. Thus, quantitative measurements of how the bronchial vessels are distributed about the airways are scarce, and quantitative data are needed to improve our understanding of bronchial circulation physiology and for incorporation into future mathematical models of airway gas exchange.

Fifteen years ago, we developed a mathematical model of soluble gas exchange in the airways (Tsu et al., 1988). Recently, we determined our model of airway gas exchange improperly described the diffusional transport of inert gases through the airway tissue (George et al., 1993). To correct this problem and properly describe the diffusion dependence in the gas exchange model, the diffusing capacity for each airway generation needed to be calculated. The diffusing capacity comes from Fick's law, describes the magnitude of gas conductance through a medium such as airway tissue and can be thought of as a mass transfer coefficient. This capacity is a function of anatomical and physiochemical parameters and can be written as:

$$D_t = \frac{D_{i,t} \cdot \beta_t \cdot A_s}{r}$$

where, $D_{i,t}$ is the molecular diffusion coefficient of a soluble inert gas i in tissue ($cm^2 \cdot sec^{-1}$) and β_t is the solubility of soluble inert gas in tissue ($mL\ gas \cdot ml\ tissue^{-1} \cdot mmHg^{-1}$), A_s is the surface area available for diffusion in the tissue (cm^2), and r is the thickness of the tissue layer (cm). To calculate a vessel's diffusing capacity through airway tissue for any soluble gas, anatomical data describing a vessel's distance from the airway lumen, r, and its surface area, A_s, needed to be specified. As a result, anatomical data on the bronchial circulation were measured.

This study demonstrates that bronchial vessels are arranged in a right-skewed distribution about sheep airways. Additionally, this study shows that the diffusing capacity of the bronchial circulation around each airway generation can be described using two parameters, (1) an effective capillary distance and (2) an effective capillary perimeter. Finally, the effective capillary distance is shown to be the sum of two lengths, (1) the first distance changes as airway diameter changes—the epithelial thickness and (2) the second distance remains constant as airway diameter changes—the effective capillary to basement membrane distance. The experimental determination of these bronchial circulation features is described in the next section.

2. Experimental methods

2.1. Animal preparation

Four adult sheep (30–36 kg) were sedated with intramuscular xylazine, intubated and mechanically ventilated. Anesthesia was maintained and deepened with sodium pentobarbital. A sternotomy was performed and pulmonary vessels were identified. A femoral artery catheter exsanguinated the animals. The lungs were removed en bloc, the heart was removed by severing of all pulmonary vessels, and the lungs were fixed with neutral buffered formalin via intratracheal instillation at 12 cmH_2O pressure (total lung capacity) overnight.

2.2. Tissue processing

One lung from each of the four animals was used for analysis. Airway samples were taken from airway generations 1–14. Airway branches were numbered progressively by generation going down the airway tree, starting with the trachea as generation zero. Airway sizes ranged from 1 to 18 mm in diameter. These airway samples were dehydrated in solutions of increasing ethanol concentrations and embedded in methyl methacrylate. Cross-sections of airways were microtomed to a thickness of 5 μm. Sections were mounted on slides for measurement and stained with Lee's stain (basic fuchsin and methylene blue).

2.3. Morphometric measurements

The tissue cross-sections were examined for the distribution of bronchial vessels surrounding airways of differing diameters. Bronchial vessels lying between the basement membrane and the adventitia–alveolar border, the tissue wall area, were visually identified around each airway using a light microscope. A video camera attached to the microscope transferred the microscopic image to a Macintosh computer running the public domain software NIH Image (developed at the US National Institutes of Health and available on the Internet at http://rsb.info.nih.gov/nih-image). Bronchial vessels were visually located on the computer screen. Then each vessel's size and distance to the airway lumen was manually measured. This procedure was done for each vessel around each airway cross-section from each sheep. For the entire study, 9997 vessels were measured around the 48 tissue cross-sections examined from four sheep.

Bronchial vessels were distinguished from lymphatic vessels using the following observations. Bronchial vessels have a wall that is thicker and more prominent than the thin wall of the lymphatic vessels. The nuclei of the bronchial endothelial cells, although flattened, are more prominent, more plump and more numerous. Almost all of the bronchial vessels contain blood cells and very few are entirely void of media ($< 3\%$). The surface geometry of the two types of vessels is significantly different. Placing the observer inside the vessel looking out, the bronchial vessels have only a concave surface geometry while the lymphatic vessels have some convex surfaces instead of all concave surfaces.

For each cross-section, morphometric measurements were made on the airway, the bronchial vasculature surrounding the airway, and the tissue surrounding the airway (Fig. 1). The two measurements made on the airway were, (1) airway major and minor axes as defined by the luminal border of the airway epithelium and (2) airway perimeter as defined by the luminal border of the airway epithelium. The luminal border was used to determine airway diameter instead of the epithelial basement membrane because calculations of convective and diffusive gas transport in the

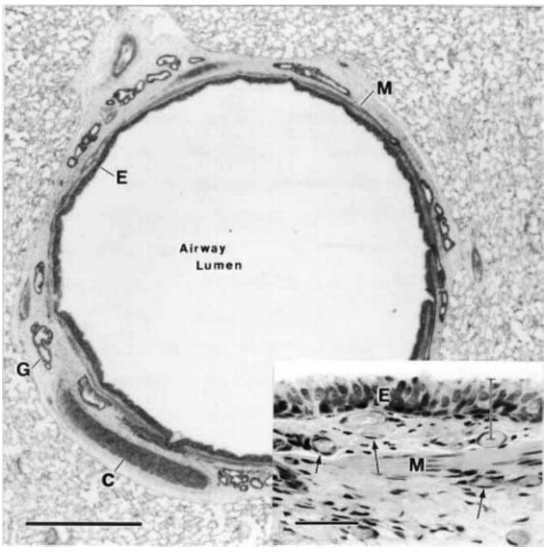

Fig. 1. Photomicrograph of a 3 mm diameter sheep airway showing the airway epithelium (E), cartilage (C), mucous gland (G), muscle (M), and surrounding alveoli. The inset is a higher magnification view of the airway epithelium and underlying histological structure. The arrows point to several of the capillaries in this field of view; they can be readily identified since nearly all are filled with red blood cells. The line segment joining the middle of one vessel to the airway lumen demonstrates how the vessel distance was measured. Length scale of the bar = 500 μm; for the inset, the length scale = 50 μm.

airways requires luminal airway diameter. This measurement correctly reflected the airway diameter in this study because, in 45 of the 48 airways the luminal border was void of tissue invaginations. Additionally, the epithelial thickness was a well-characterized function of airway diameter and as a result the epithelial basement membrane perimeter can be accurately calculated from the luminal border perimeter. To describe the bronchial vessels, three measurement were made, (1) shortest distance from the airway lumen to the center of each bronchial vessel; (2) major and minor axes of each bronchial vessel; and (3) perimeter of each bronchial vessel as defined by the luminal border of the vessel endothelium (Fig. 1). Two measurements were made on airway tissue. The epithelial thickness, the distance between the airway lumen and the epithelial basement membrane, was measured at more than 30 equally spaced locations around each airway. The size of the airway wall, the shortest distance between the epithelial basement layer and the alveolar boundary, was measured at more than 20 equally spaced locations around each airway.

These measurements were used to calculate the following for both airways and bronchial vessels, (1) cross-sectional area; (2) perimeter; and (3) diameter. For vessels, the cross-sectional area was used to calculate an equivalent diameter of a circle of equal cross-sectional area. From this diameter, a capillary was defined as a bronchial vessel with an equivalent diameter less than or equal to 10 μm as defined by Mariassy et al. (1991). All other bronchial vessels were categorized as arterioles/venules (i.e. all non-capillary vessels). The epithelial thickness was calculated to be the average of 30 or more measurements made around each airway. Additionally, the total wall tissue area was defined as the tissue area between the epithelial basement layer and the alveolar boundary. The total wall tissue area was calculated by numerical integration of the measured distances (epithelial basement membrane to alveolar boundary) using the trapezoid rule. Since 20 or more measurements were taken, we felt the error in the calculated tissue area was small ($<$ 10%).

2.4. Data analysis

The measurements were made so that for a given airway, the contribution of gas transferred from the bronchial circulation to that airway could be determined. In order to calculate the gas transferred, it is necessary to sum the diffusional contribution from each vessel near that airway. However, this calculation will not be valid for every situation. If any of the parameters governing diffusion changed (i.e. a new inert gas or a different inert gas partial pressure), the diffusive transfer of soluble gas for each airway generation would need to be recalculated. Due to the large numbers of vessels about each airway, recalculating the diffusive transport of gas is impractical. As a result, an alternative method was chosen. For each airway, the large array of vessel sizes and vessel-to-lumen distances were reduced to two parameters, (1) an effective size; and (2) an effective distance. These reductions were done using the method of weighted averages as described below.

The weighted averages of vessel sizes and vessel-to-lumen distances were calculated by using Fick's first law as the weighting function. Fick's law for steady state diffusion of a solute from any bronchial vessel to airway lumen can be written as follows:

$$J_r(z) = -D_{i,t} \cdot \beta_t \cdot A_s \frac{\Delta P}{\Delta r} \quad (1)$$

where, $J_r(z)$, molecular diffusion rate in the z-plane of a solute in the r direction ($mL \cdot sec^{-1}$); z, axial distance into the lung from the mouth (cm); $D_{i,t}$, molecular diffusion coefficient of solute, i, in tissue ($cm^2 \cdot sec^{-1}$); β_t, solubility of solute in tissue (ml gas $\cdot$ ml tissue^{-1} $\cdot$ mmHg^{-1}); A_s, surface area of a vertical vessel (cm^2) $\Delta P/\Delta r$, radial partial pressure gradient of solute in the tissue layer between the vessel and the airway lumen surface.

If we define $\Delta r = r$, where r is the radial distance (cm) from the vessel center to the airway lumen, and define $A_s = S \times \Delta z$, where S is the perimeter of the vessel (cm) and Δz its length (cm), Eq. (1) can be rewritten:

$$J_r(z) = -D_{i,t} \cdot \beta_t \cdot S \cdot \Delta z \frac{\Delta P}{r} \quad (2)$$

where, the grouping of variables $D_{i,t}$, Δz, β_t, S, and r are equal to the diffusing capacity, D_t, as defined previously. Rearranging Eq. (2), we obtain the following, valid for any bronchial vessel:

$$\frac{S}{r} = \frac{J_r(z)}{D_{i,t} \cdot \beta \cdot \Delta z \cdot \Delta P} \quad (3)$$

If we further assume that Δz, ΔP, β_t, and $D_{i,t}$ are constant, then Eq. (3) becomes:

$$\frac{S}{r} = -\frac{J_r(z)}{K} \quad (4)$$

where, $K = D_{i,t} \cdot \beta_t \cdot \Delta z \cdot \Delta P$.

Since, $J_r(z)$ is a function of z only, S/r is a measure of the diffusing capacity of the bronchial vessel. For each vessel i, this measure can be defined as follows:

$$\gamma_i = \frac{S_i}{r_i} \quad (5)$$

Now, to obtain a weighted distance of a vessel from the lumen, consider a number weighted average described by:

$$\bar{r} = \frac{\sum n_i r_i}{\sum n_i}$$

where, n_i is the number of vessels a distance r_i from the lumen. In this study, this measure of diffusing capacity, γ_i, is used as the weighting function so that the weighted average becomes:

$$\bar{r} = \frac{\sum \gamma_i r_i}{\sum \gamma_i} \quad (6)$$

Since $\gamma_i = S_i/r_i$, an effective distance, $\bar{r}$, is defined as:

$$\bar{r} = \frac{\sum S_i}{\sum S_i/r_i} \quad (7)$$

In a similar manner, an effective perimeter, $\bar{S}$, can be defined as:

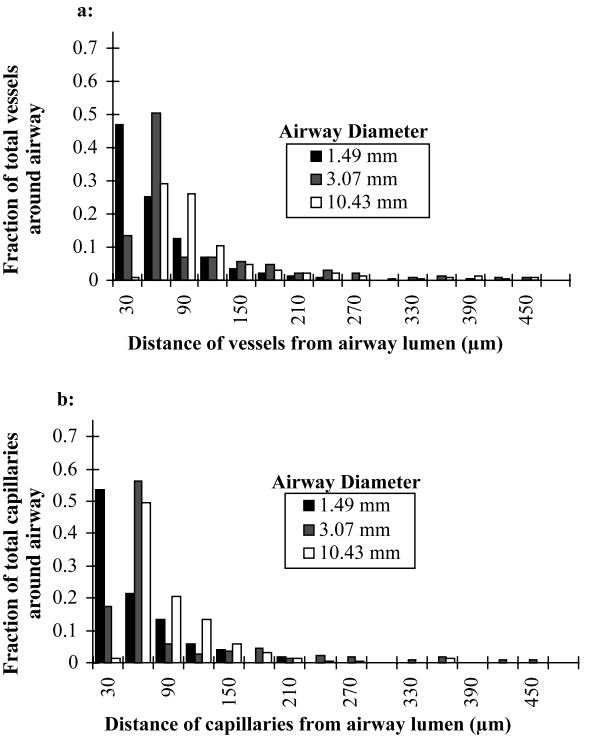

Fig. 2. The radial distribution of bronchial vessels from the airway lumen is similar to a right-skewed distribution. The distributions of bronchial vessels around three representative airways (d = 1.49 mm, 3.07 mm, and 10.43 mm) from sheep 3 are plotted. The distribution of all vessels (capillaries, venules, and arterioles) around the three representative airways are plotted in panel a whereas panel b displays the distribution of capillaries only (minor axes ≤ 10 μm). Notice that most vessels lie near the airway lumen. However, bronchial vessels around large airways lie, on average, further from the airway lumen than bronchial vessels around smaller airways.

$$\bar{S} = \bar{r} \sum \gamma_i \quad (8)$$

3. Results

3.1. Bronchial vessel distribution

Using the vessel data, we found the bronchial vessels to be arranged in a right-skewed distribution about the bronchial airways (Fig. 2a). The right-skewed distribution has three notable char-

acteristics, (1) a steep leading edge; (2) a gentle sloping tail; and (3) a lack of symmetry about its mean. Since the distribution of bronchial vessels conforms to a right-skewed distribution, we can conclude that most vessels are located close to the airway lumen. Of those vessels that are spatially near the airway lumen, most are smaller vessels (i.e. capillaries) whereas the vessels that are distant from the lumen are generally larger in size, arterioles or venules. This trend can be seen by comparing the peak of the distributions in Fig. 2b with the corresponding peak in Fig. 2a and realizing that more than 80% of the vessels surrounding the airways are capillaries.

This right-skewed distribution was valid for airways of different diameters. However, for larger airways the shape of this distribution seemed to flatten out with a more gradual leading edge and a longer trailing edge (Fig. 2a). Thus, bronchial vessels around large airways lie, on average, further from the airway lumen than bronchial vessels around smaller airways.

3.2. Epithelial layer and lumen–alveolar thickness

For each sheep, a best-fit line was determined for the following relationships, (1) the airway epithelial thickness versus airway diameter; and (2) the lumen–alveolar thickness versus airway diameter. The slope, intercept, and r^2 for each of these best-fit lines are given in Table 1. The average best-fit parameters were calculated for sheep 1–3. Sheep 4 was excluded from the average values because its epithelial thickness decreased with increasing airway diameter, which was the opposite trend of the other three sheep (see Fig. 3). We felt this result was a consequence of an airway pathology in sheep 4 which we subsequently investigated (Section 4).

3.3. Tissue wall area and vessel area

Wagner and Mitzner (Wagner and Mitzner, 1996) have shown a linear relationship between the square root of the airway wall area and the airway diameter (d). In a similar analysis, the square root of the wall area and capillary cross-sectional area were regressed against airway diameter. The slopes, intercepts and r^2 values from this regression are given in Table 2 for each sheep. An average value of the slope, intercept and r^2-value for sheep 1–3 is presented in Table 2. Sheep 4 is excluded from the average because of a possible airway pathology.

3.4. Diffusion weighted parameters

The method of diffusion-weighted averages as described in Section 2.4 was used to assist in quantifying soluble gas diffusion from the bronchial circulation to the airway lumen. This analysis was done for each sheep using only capillary vessels (diameter ≤ 10 μm). The diffusion weighted capillary distance (effective distance) and diffusion weighted capillary perimeter (effective perimeter) were regressed against airway diameter. The results of this regression (i.e. slope, intercept and r^2-value) for each animal are presented in Table 3. Again, an average value of the slope, intercept and r^2-value are presented for sheep 1–3 only because sheep 4 was suspected to have an airway pathology.

Fig. 3 presents plots of effective distance and epithelial thickness for each sheep versus airway

Table 1
Epithelial thickness and lumen–alveolar distance

Sheep	M	B	r^2	*N*
Epithelial thickness				
1	0.00153	0.0021	0.56	11
2	0.00071	0.0017	0.64	13
3	0.00219	0.0029	0.79	11
4	−0.00089	0.0035	0.50	13
Average 1–3	0.00147	0.0022	0.66	
Lumen–alveolar thickness				
1	0.0647	0.0104	0.89	11
2	0.0973	−0.0016	0.97	13
3	0.0951	0.0079	0.92	10
4	0.0696	0.0114	0.88	13
Average 1–3	0.0847	0.0056	0.93	

Parameters for best fit line through data on epithelial thickness and lumen–alveolar distance for all four sheep. The best fit line has the form y (cm) = m × d (cm) + b, where, d is airway diameter. *N* is the number of airways sampled, r^2 refers to the goodness of fit. Sheep 4 is excluded from the parameter average because of suspected airway inflammation.

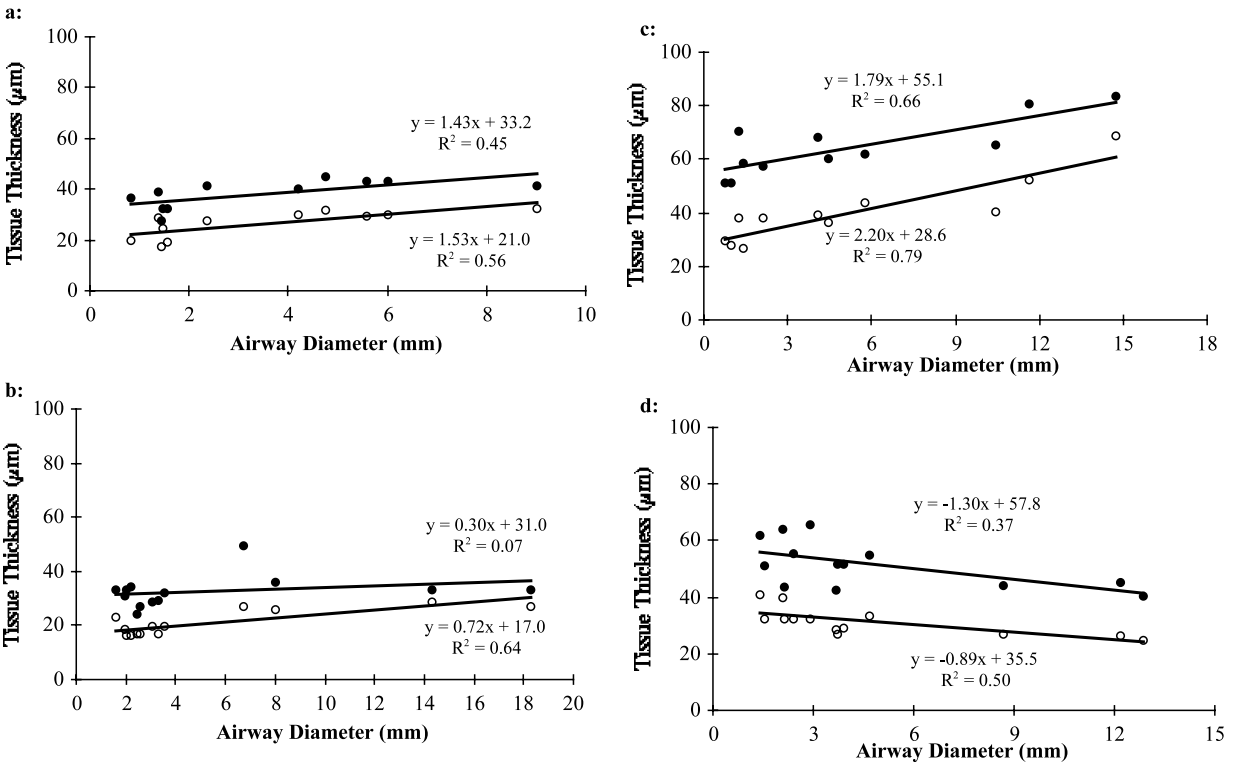

Fig. 3. Effective capillary distance (solid circles, ●) and epithelial thickness (open circles, ○) are plotted against airway diameter for sheep 1 (Panel a), sheep 2 (Panel b), sheep 3 (Panel c), and sheep 4 (Panel d). A best fit line is shown (solid black) for both sets of data. A statistical analysis has shown the difference between effective capillary distance and epithelial thickness is invariant with airway diameter. Notice tissue thickness (epithelial and capillary) decreases with airway diameter for sheep 4 (Panel d). This trend is thought to be a result of an airway pathology.

diameter along with their respective best-fit lines. An F-test was used to show that the slope of each best-fit line was different than zero ($P < 0.05$) with the exception of the effective distance line for sheep 2 (Fig. 3b). Notice that the effective distance and epithelial thickness increase with increasing airway diameter for sheep 1–3 (panel a–c). For sheep 4 (panel d), both the effective distance and epithelial thickness decreased with airway diameter, a sharp contrast to the trends of the other three sheep. This was the first indication of an airway pathology for sheep 4.

We hypothesized that the effective capillary distance could be divided into two lengths - one that changes with airway diameter and another that remains constant with airway diameter. Examining each panel in Fig. 3, the best fit lies for the effective distance and epithelial thickness data appeared to change in the same manner with airway diameter. In other words, the slopes of these two lines looked to be equivalent. From this observation, we hypothesized that the component of the effective capillary distance that varied with airway diameter was the epithelial thickness, the distance from the airway lumen to the epithelial basement membrane; the constant component of the effective capillary distance was the capillary to basement membrane distance. To test these hypotheses, two statistical analyses were performed. First, using a complex regression model (Mendenhall and Sincich, 1995), we demonstrated ($P < 0.05$) that the slopes of the effective distance and epithelial thickness versus airway diameter were statistically equivalent within each sheep (including sheep 4). This means that changes in effective capillary distance with airway diameter are caused

by changes in epithelial thickness as hypothesized. Second, epithelial thickness data were subtracted from their corresponding effective distance data resulting in data describing the capillary to epithelial basement membrane distance, hypothesized to be constant with airway diameter. Using a simple linear model, this capillary to epithelial basement membrane distance was regressed against airway diameter. An F-test was used to show that the slope of this line is statistically zero ($P < 0.05$) for each sheep (including sheep 4). Thus, our hypothesis that capillary to basement membrane distance is constant was verified. In summary, the effective capillary distance can be described as the sum of two lengths - one that changes with airway diameter and another that remains constant with airway diameter.

4. Discussion

4.1. Vessel distribution

The results demonstrated that most capillaries (vessels ≤ 10 μm in diameter) lie within the first 100 μm of the airway lumen. Similarly, Laitinen et al. (Laitinen et al., 1989) observed, in dogs, that capillaries (vessels 4–10 μm in diameter) mainly occupy the first 100 μm of tissue from the epithelial basement membrane. The proximity of these exchange vessels to the airway lumen allows them to play an active role in lung fluid balance and the humidification of the airways. In addition, the bronchial circulation plays an important role in the exchange of highly soluble gases (Schrikker et al., 1985). This exchange process is diffusion dependent (Swenson et al., 1992). One of the parameters that limits the diffusing capacity of the bronchial capillaries is the distance of the capillaries from the airway lumen which, as these results show, is determined by the thickness of the epithelial layer. Thus, changes in the epithelial tissue thickness may significantly alter the rate of airway gas exchange.

Data have previously been published on the epithelial thickness in sheep for five airway generations (Chen et al., 1991). In formalin fixed tissue

Table 2
Tissue wall and capillary cross-sectional area

Sheep	m	B	r^2	*N*
Square root of the tissue wall area				
1	0.518	0	0.96	11
2	0.556	0	0.99	13
3	0.589	0	0.98	10
4	0.522	0	0.96	13
Average 1–3	0.554	0	0.97	
Square root of the capillary area				
1	0.0127	0.0040	0.79	11
2	0.0079	0.0037	0.97	13
3	0.0149	0.0013	0.99	11
4	0.0096	0.0026	0.81	13
Average 1–3	0.0118	0.0030	0.91	

Parameters for best fit line through data on tissue wall area and capillary area for all four sheep. The best fit line has the form y (cm) = m × d (cm) + b, where, y is the square root of the cross-sectional area and d is airway diameter. *N* is the number of airways sampled, r^2 refers to the goodness of fit. Sheep 4 is excluded from the parameter average because of suspected airway inflammation.

Table 3
Effective capillary distance and perimeter for each airway diameter were calculated from the method of diffusion weighted averages (Eqs. (7) and (8))

Sheep	M	b	r^2	*N*
Effective distance				
1	0.0014	0.0033	0.44	11
2	0.0003	0.0031	0.07	13
3	0.0018	0.0055	0.70	11
4	−0.0013	0.0058	0.37	13
Average 1–3	0.0012	0.0040	0.40	
Effective perimeter				
1	1.87	0	0.74	11
2	1.55	0	0.96	13
3	2.06	0	0.94	11
4	1.47	0	0.91	13
Average 1–3	1.83	0	0.88	

Parameters for best fit line through effective distance and perimeter for all four sheep are tabulated. The best fit line has the form y (cm) = m × d (cm) + b, where, d is airway diameter. *N* is the number of airways sampled, and r^2 refers to the goodness of fit. Sheep 4 is excluded from the parameter average because of suspected airway inflammation.

cross-sections, the epithelial thickness was between ~55–65 μm for bronchial airways and approximately 30 μm for bronchioles. Accordingly, the epithelial thickness increased with airway diameter. Those measurements of epithelial thickness agree with the values presented here.

4.2. Health of sheep 4

Sheep 4 has been excluded from our analysis because, it presented two signs of pathology. First, an examination of the epithelial thickness for sheep 4 revealed that the epithelial thickness and effective capillary distance decreased with increasing airway diameter (Fig. 3d). This trend is not supported by the other three sheep (Fig. 3a–c) where epithelial thickness and effective capillary distance increased with airway diameter. Additionally, the literature shows epithelial thickness to increase with airway diameter in both sheep (Chen et al., 1991) and humans (Gastineau et al., 1972; Mercer et al., 1991) in sharp contrast to the data from sheep 4. Second, we examined the tissue cross-sections of sheep 4 under light microscopy. In particular, the examination focused on the epithelial cell layer since changes in this layer were shown to determine changes in effective capillary distance for all four sheep (Section 3Fig. 3). The goblet cells in the epithelial layer of sheep 4 were found to have hypertrophied. Although abnormalities in other cell lines were not identified under the microscope, the hypertrophied goblet cells are believed to be a marker of an inflammatory process probably localized within a region of the airways but not limited to only goblet cells (Zhu et al., 1999). We speculated that this condition was a result of a chronic exposure to an environmental antigen, but we were unable to precisely verify this suspicion. Due to this finding and the abnormal trend in epithelial thickness, sheep 4 was believed to have airway pathology at the time of the study. Since we were unable to precisely determine the cause of airway pathology, sheep 4 was not eliminated from the study, but rather it was excluded from our analysis and from the averages of the regression parameters.

4.3. Tissue shrinkage

We chose our method of fixing and processing the lung tissue because, we felt it would minimize tissue shrinkage. To determine the extent of tissue shrinkage, a few airways were selected and their diameters were measured three times, (1) post-fixation; (2) post dehydration; and (3) post embedding. For each airway, all three measurements were within 1% of one another. As a result we, did not feel it necessary to account for the effect of tissue shrinkage on our measurements.

4.4. Predicting airway gas exchange using measured parameters

The measurements made on the bronchial circulation as described in Section 2 will be used to improve a mathematical model of airway gas exchange (George et al., 1993). Four parameters calculated from these data are needed to update and improve the description of the bronchial circulation within the model. The first two of those parameters are the effective capillary perimeter and the effective capillary distance. Utilizing these two parameters, the bronchial diffusing capacity can be completely specified since the molecular diffusion coefficient of a soluble gas in tissue and tissue solubility of a soluble gas is fairly well defined. A third parameter, lumen–alveolar distance, will help specify the diffusing capacity of soluble gas from pulmonary capillaries lying just distal to the adventitia of intraparenchymal airways. The fourth parameter, capillary volume, will be calculated from the capillary cross-sectional area. This parameter will improve the description of the perfusion dependence of airway gas exchange on the bronchial circulation. It is important to note that capillary volume cannot be calculated from the diffusion weighted (effective) perimeter as this perimeter overestimates the capillary volume.

By scaling these sheep parameters, gas exchange calculations in human lungs can be made. The sheep parameters can be normalized by a second sheep tissue measurement. This second measurement should have two qualities, (1) a similar functionality with airway diameter as the first and

(2) a corresponding measurement in humans. For example, capillary to lumen (effective) distance can be normalized by epithelial thickness in sheep (Tables 1 and 3). To determine capillary to lumen distance in humans at total lung capacity, the normalized distance should be multiplied by epithelial thickness in humans. Multiplying this dimensional distance in humans by $(V/V_{TLC})^{1/3}$, the distance can be rescaled to the appropriate lung volume, V.

4.5. Capillary surface to volume ratio and airway surface to volume ratio

The efficiency of gas exchange in the airways has been shown to be dependent on airway surface area to airway volume ratio (Hu et al., 1992). Likewise, the efficiency of gas exchange with the bronchial circulation is dependent on the capillary surface area to capillary volume ratio (S/V). Using four representative airway diameters, S/V values were calculated for bronchial capillaries using two average best-fit lines, (1) effective capillary perimeter (Table 3); and (2) capillary cross-sectional area (Table 2). These bronchial capillary S/V values are presented with S/V values for sheep airways $(4/(\pi \cdot d))$ in Table 4. For small airways, S/V was large for both airways and bronchial capillaries but S/V decreased with increasing airway size. The S/V for the bronchial circulation in sheep was generally 20–30 times larger than the S/V of the airways (see Table 4, ratio). Additionally, the ratio of bronchial capillary surface area to airway surface area was calculated as 0.58 and independent of airway diameter. Since bronchial capillary gas exchange generally implies gas exchange with the airways, the bronchial surface area actually participating in gas exchange with the airways is half of the total capillary surface area. The other half of the capillary surface faces the adventitia–alveolar boundary (Fig. 1). So in terms of airway gas exchange, S/V for the bronchial circulation in sheep is 10–15 times larger than the S/V of the airways and the ratio of capillary to airway surface area is 0.29.

5. Conclusions

The axial and radial distribution of bronchial vessels has been determined to quantify the diffusing capacity of the bronchial circulation. The bronchial vessels surrounding airways were found to be radially dispersed in a right-skewed distribution. Capillaries (vessels ≤ 10 μm) mainly reside within the first 100 μm of airway tissue. Additionally, bronchial capillary diffusing capacity for each airway was described by two parameters, (1) effective capillary distance and (2) effective capillary perimeter. The effective capillary distance was shown to be the sum of two lengths, (1) the first length changes as airway diameter changes—the epithelial thickness; and (2) the second distance remains constant as airway diameter changes—the capillary to basement membrane distance. The surface area to volume ratio of the bronchial capillaries was 20–30 times greater than that of the airway themselves. These bronchial circulation data will be used to improve a model of airway gas exchange to describe the diffusion of inert gases through the airway tissue and the

Table 4
Surface area to volume ratio (S/V) for sheep airways and bronchial capillaries

Airway diameter (cm)	Bronchial capillary (S/V)	Airway (S/V)	Ratio of Br. Cap. to Airway (S/V)
0.1	830	40	20.7
0.5	236	8	29.5
1.0	124	4	31.0
1.5	84	2.6	31.5

For a given airway diameter (cm), the bronchial capillary S/V surface area to volume ratio is 20–30 times greater than the surface to volume ratio of the airways (see Ratio column). The ratio of capillary surface area to airway surface area is 0.5816 and independent of airway diameter.

perfusion of airway tissue via the bronchial circulation.

Acknowledgements

This work was supported, in part, by grant HL24163 from the National Heart, Lung, and Blood Institute. We thank Dr Bret Snyder and Professor Jacob Hildebrandt for their valuable discussion and critiques, and John C. Boykin for his technical assistance.

References

Baile, E.M., Dahlby, R.W., Wiggs, B.R., Paré, P.D., 1985. Role of tracheal and bronchial circulation in respiratory heat exchange. J. Appl. Physiol. 58, 217–222.

Charan, N.B., Carvalho, P., 1997. Angiogenesis in bronchial circulatory system after unilateral pulmonary artery obstruction. J. Appl. Physiol. 82, 284–891.

Charan, N.B., Turk, G.M., Dhand, R., 1984. Gross and subgross anatomy of bronchial circulation in sheep. J. Appl. Physiol. 57, 658–664.

Charan, N.B., Baile, E.M., Pare, P.D., 1997. Bronchial vascular congestion and angiogenesis. Eur. Resp. J. 10, 1173–1180.

Chen, W., Alley, M.T., Manktelow, B.W., 1991. Morphological and morphometric studies of the airways of sheep with acute airway hypersensitivity to inhaled Ascaris suum. Int. J. Exp. Path. 72, 543–551.

Cudkowicz, L., 1992. In: Butler (Ed.), The Bronchial Circulation. Marcel Dekker, New York, pp. 3–41.

Deffebach, M.E., Charan, N.B., Lakshminarayan, S., Butler, J., 1987. The bronchial circulation: small, but a vital attribute of the lung. Am. Rev. Respir. Dis. 135, 463–481.

Gastineau, R.M., Walsh, P.J., Underwood, N., 1972. Thickness of the bronchial epithelium with relation to exposure to radon. Health Phys. 23, 857–860.

George, S.C., Babb, A.L., Hlastala, M.P., 1993. Dynamics of soluble gas exchange in the airways. III. Single-exhalation breathing maneuver. J. Appl. Physiol. 75, 2439–2449.

Hill, P., Goulding, D., Webber, S.E., Widdicombe, J.G., 1989. Blood sinuses in the submucosa of the large airways of the sheep. J. Anat. 162, 235–247.

Hu, S.C., Ben-Jebria, A., Ultman, J.S., 1992. Simulation of ozone uptake distribution in the human airways by orthogonal collocation on finite elements. Comp. Biomed. Res. 25, 264–278.

Laitinen, A., Laitinen, L.A., Moss, R., Widdicombe, J.G., 1989. Organisation and structure of the tracheal and bronchial blood vessels in the dog. J. Anat. 165, 133–140.

Magno, M.G., Fishman, A.P., 1982. Orgin, distribution, and blood flow of bronchial circulation in anesthetized sheep. J. Appl. Physiol. 53, 272–279.

Mariassy, A.T., Gazeroglu, H., Wanner, A., 1991. Morphometry of the subepithelial circulation in sheep airways. Am. Rev. Respir. Dis. 143, 162–166.

Mendenhall, W., Sincich, T., 1995. Statistics for Engineering and the Sciences. Prentice-Hall, Upper Saddle-River.

Mercer, R.R., Russell, M.L., Crapo, J.D., 1991. Radon dosimetry based on the depth distribution of nuclei in human and rat lungs. Health Phys. 61, 117–130.

Pump, K.K., 1972. Distribution of bronchial arteries in the human lung. Chest 62, 447–451.

Rizk, N.W., Luce, J.M., Price, D.C., Murray, J.F., 1984. Site of deposition and factors affecting clearance of aerosolized solute from canine lungs. J. Appl. Physiol. 56, 723–729.

Schraufnagel, D.E., Pearse, D.B., Mitzner, W.A., Wagner, E.M., 1995. Three-dimensional structure of the bronchial microcirculation in sheep. Anat. Rec. 243, 357–366.

Schrikker, A.C.M., d. Vries, W.R., Zwart, A., Luijendijk, S.C.M., 1985. Uptake of highly soluble gases in the epithelium of the conducting airways. Pflugers Arch. 405, 389–394.

Swenson, E.R., Robertson, H.T., Polissar, N.L., Middaugh, M.E., Hlastala, M.P., 1992. Conducting airway gas exchange: diffusion related differences in inert gas elimination. J. Appl. Physiol. 72, 1581–1588.

Tsu, M.E., Babb, A.L., Ralph, D.D., Hlastala, M.P., 1988. Dynamics of heat, water and soluble gas exchange in the human airways: 1. a model study. Ann. Biomed. Eng. 16, 547–571.

Wagner, E.M., Mitzner, W., 1996. Effects of bronchial vascular engorgement on airway dimensions. J. Appl. Physiol. 81, 293–301.

Zhu, Z., Homer, R., Wand, Z., Chen, Q., Geba, G., Wang, J., Zhang, Y., Elias, J., 1999. Pulmonary expression of interleukin-13 causes inflammation, mucus hypersecretion, subepithelial fibrosis, physiologic abnormalities, and eotaxin production. J. Clin. Invest. 103, 779–788.